ISSN: 1999-1630

SEU Journal of Science and Engineering, Vol. 13, No. 1, June 2019

A Novel Performance Augmentation Strategy for Type 4 Wind Generator Systems under Voltage Sags and Swells

Tapash Kumar Das[1]

[1]*Electrical and Electronic Engineering Department, Southeast University, Dhaka, Bangladesh, E-mail: tapash54@gmail.com*

Abstract

Type 4 wind generator systems need to continue their connection to the power grid in the occurrence of voltage fluctuations to meet modern grid code requirements. Wind generators also have to inject or absorb sufficient reactive current into or from the grid to maintain voltage stability. However, Type 4 wind generator systems require extra safeguard during grid voltage fluctuations because of the undesirable overvoltage in the dc-link capacitor leading to converter deterioration. This paper proposes an innovative performance augmentation strategy for Type 4 wind generators subjected to voltage fluctuations in the form of sags and swells. The disturbances happen at PCC (Point of Common Coupling). The strategy includes a safety scheme and a reactive power regulation scheme operating in coordination. The coordination is maintained by a supervisory controller. The safety scheme safeguards the Type 4 wind generator converter by limiting the dc-link capacitor voltage within satisfactory bounds, while the reactive power regulation augments the PCC voltage by regulating the flow of reactive power as a function of the PCC voltage. A neural network predictive controller (NNPC) is also designed as part of the power management scheme to improve dc-voltage regulation. Also, it has the added advantage of enhanced performance when the mechanical system is exposed to disturbance. It is established that the operation of the Type 4 wind farm is enhanced considerably with the presented strategy. A 10-MW WRSG grid-connected wind farm is utilized for simulation in MATLAB/Simscape Power Systems to verify the efficacy of the augmentation strategy.

Keywords: Type 4 wind generator, voltage fluctuation, ride-through enhancement, reactive power regulation, neural network predictive control

I. Introduction

A large portion of the global renewable energy can be attributed to wind power and its part in energy production will increase even more in the future (P. Beiter *et al.*, 2015). The significant participation of wind energy in electric utility grids contributed to a change in modern grid code requirements (F. Valenciaga *et al.*, 2015). Wind power generators have to continue their connection with the power grid in the event of voltage sags and swells; they are also required to control reactive power movement to and from the PCC for stability enhancement. This presents some issues for Type 4 wind generator systems, which currently offer the latest wind technology. Voltage sags and swells bring about an overvoltage of the dc-link capacitor (J.F. Conroy *et al.*, 2007). This can harm the wind generator full-scale converter and they need to be protected during grid voltage fluctuations. Furthermore, wind generators have to maintain voltage stability. A systematic review of the present literature related to ride-through schemes of Type 4 wind systems is given below.

Some work has been done on developing ride-through strategies of Type 4 wind generators which is the latest configuration in wind generator technology. The solutions for ride-through enhancement can be divided into three types. The first type includes the implementation of advanced controllers for ride-through performance improvement. In A. Mullane *et al.*, (2005), a nonlinear controller is designed using feedback linearization for current and dc-link voltage control to enhance ride-through. Feedback linearization is again used in K.H. Kim *et al.*, (2012) for dc-link voltage control during grid symmetrical and asymmetrical voltage sags.

* **Corresponding Author:** Dr. Tapash Kumar Das, Assistant Professor, Department of Electrical and Electronic Engineering, Southeast University, 251/A & 252 Tejgaon I/A, Dhaka, Bangladesh; E-mail: *tapash54@gmail.com*

In this paper, sequence decomposition is implemented for current reference generation in the positive and negative components separately. Three different Linear Quadratic Regulators (LQR) are designed in S. Alepuz *et al.*, (2009) for current control during asymmetrical voltage sags to improve ride-through performance. The regulators are based on symmetrical components and the choice of controllers is determined by system constraints and performance criteria. In (F. Valenciaga *et al.*, 2015), a Multiple-Input-Multiple-Output (MIMO) sliding mode controller is proposed to enhance LVRT performance by controlling dc-link voltage, active power, reactive power and current for symmetrical voltage sags. Parametric variation and external perturbation are also investigated. The authors in H. M. Yassin *et al.*, (2016) propose a fuzzy controller to control dc-link voltage for low voltage ride through (LVRT) enhancement. The generator speed is related nonlinearly to the dc-link voltage and this is taken into account for controller design.

The second category of solutions involves modification to conventional vector control to enhance ride-through. In A.D. Hansen *et al.*, (2009), traditional vector control is modified to provide uninterrupted operation and a dc-link chopper protects the dc-link capacitor. An integrated dc-link current control is presented in (J. Dai *et al.*, 2011) to coordinate the generator side and grid side converters for enhanced ride-through capability. In H. Geng *et al.*, (2011), an integrated power control scheme is presented where the generator-side converter regulates the dc-link voltage; while the grid side converter regulates the power flow between the grid and generator. Both symmetrical and asymmetrical grid voltage sags are investigated. A technique is presented in S. Alepuz *et al.*, (2013) to accumulate additional active power in the shaft of the wind generator for LVRT. However, a dc-link chopper circuit is still employed for protection. A reference generation strategy is designed in V. Yaramasu *et al.*, (2014) to store surplus energy in rotor inertia during low voltages. A model predictive controller (MPC) controller is also employed. The objectives of the controller are attained by minimisation of certain cost functions. Only asymmetrical voltage sags are considered in T. Neumann *et al.*, (2015) where sequence decomposition is utilised to design LVRT control strategy. Three different solutions are explored and their performance is expounded on.

The third and final type entails the implementation of hardware for ride-though augmentation. A combination of Energy Storage System (ESS) and dc-link chopper is utilised in T.H.Nguyen *et al.*, (2013). The ESS is controlled using a separate converter which raises the overall price of the system. In M. Popat *et al.*, (2013), cascaded converters are used on the generator side and grid side to enhance performance. Reactive power augmentation is also provided but only symmetrical voltage sags are considered in the strategy. In G. Ramtharan *et al.*, (2009) two current controllers are presented based on symmetrical components to counter symmetrical and asymmetrical voltage sags. The authors propose performance enhancement utilizing high voltage AC and high voltage DC transmission systems connected to offshore wind generators. A chopper circuit in the DC-link is employed here as well. In Akhmatov, (2006), the Type 4 converter is manipulated using certain blocking and restart sequences to improve ride-through capability. During voltage sag, the generator-side converter is bypassed but the grid-side converter keeps working to support the PCC voltage. The generator-side converter is restarted and reconnected to the grid when the disturbance is cleared. The authors propose a mixed wind farm topology in S.M.Muyeen *et al.*, (2010). The topology consists of fixed-speed (Type 1) wind generators connected in series and in parallel to Type 4 wind generators. This enhances the LVRT capability of both types of wind generators. It should be noted that several afore-mentioned papers use a mixture of the three solution categories.

All the proposed solutions only partially improve the grid-code requirements for Type 4 wind generators. As wind power penetration rises, modern grid codes stipulate a comprehensive performance augmentation strategy that encompasses both sags and swells, moreover helps retain voltage stability of the grid M. Tsili *et al.*, (2009). This paper presents such an all-inclusive strategy for Type 4 wind

generators to protect the converter in all scenarios and effectively manage the flow of reactive power between the grid and wind generator. The scheme also provides an additional functionality of improved performance when the mechanical system is exposed to disturbance. This will facilitate a high penetration of wind power in the grid.

II. Type 4 wind power generator

The quantity of power obtainable from wind is shown by (1); where ρ is air density, A represents the cross-sectional area of generator turbine and v symbolizes the wind speed. Yet, the generator turbine can only absorb a certain percentage of the total energy present in wind. The quantity of wind power absorbed by the generator turbine is shown in (2). C_p is the power coefficient and it is calculated using the tip-speed ratio, λ , and the blade angle, β. The association in (3) between C_p and β is extremely nonlinear and is frequently supplied by the manufacturer. The equation for λ is symbolized by (4). The turbine radius is r and ω_t represents the rotor mechanical speed.

$$P_{from\_wind}=(1/2)\,\rho A v^3 \quad (1)$$

$$P_{extracted\_from\_wind} = C_p \, x \, P_{wind} \quad (2)$$

$$C_p=f(\lambda, \beta) \quad (3)$$

$$\lambda = \omega_t r/v \quad (4)$$

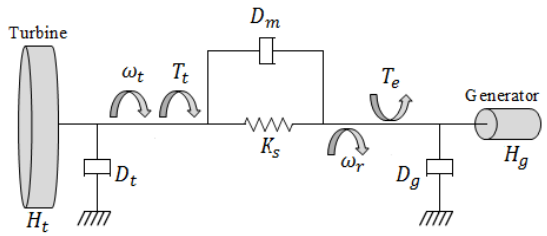

Figure 1: Mechanical system of a wind generator

A two-mass model of the wind turbine shown in Fig. 1 is utilised for the wind power system. This model is sufficient for power system analysis. The mechanical system can also be designed as a three-mass or one-mass model. However, the three-mass model is too detailed which is unnecessary for this work; whereas, the one-mass model is overly simplified.

The two-mass model consists of two inertias: the turbine inertia (H_t) and the generator inertia (H_g). The turbine inertia represents the sum of inertias of the turbine, part of the gearbox and low-speed shaft, while the generator inertia incorporates the mass of the rotor, part of the gearbox and high-speed shaft. The two inertias are connected by a shaft with a stiffness coefficient of K_s. T_t and ω_t are mechanical torque and speed respectively; whereas, T_e and ω_r symbolise electrical torque and speed in that order. The three damping coefficients are the turbine damping coefficient (D_t), the generator damping coefficient (D_g), and the mutual damping (D_m). D_t symbolises the aerodynamic resistance of the turbine blade, D_g represents mechanical friction and windage; finally, D_m is the impact of the difference in speed between the rotor and the turbine. Equations (5)-(8) define the mechanical structure of the wind generators.

$$2H_t d\omega_t/dt = T_t - K_s(\theta_r-\theta_t) - D_m(\omega_r-\omega_t) \quad (5)$$

$$2H_g d\omega_r/dt = -Te + K_s(\theta_r-\theta_t) + D_m(\omega_r-\omega_t) \quad (6)$$

$$d\theta_t/dt = \omega_t \quad (7)$$

$$d\theta r/dt = \omega_r \quad (8)$$

The electrical arrangement of the synchronous wind generator is presented in (9)-(14) in the rotor d-q reference frame. The symbols ‘k’, ‘s’, ‘f’, ‘d’ and ‘q’ represent, damping, stator, field, d-axis and q-axis components in that order. V, I, R and Ψ represent voltage, current, resistance and flux respectively. The electromagnetic torque that links the electrical system to the mechanical system is given in (15). The full-scale converter can handle 100% of the rated power output of the wind generator.

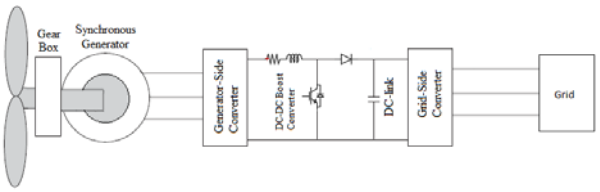

Figure 2: Type 4 WRSG configuration

$$V_{ds} = R_s I_{ds} + d\psi_{ds}/dt - \omega_r \psi_{qs} \quad 9$$

$$V_{qs} = R_s I_{qs} + d\psi_{qs}/dt + \omega_r \psi_{ds} \quad 10$$

$$V_{fd} = R_{fd} I_{fd} + d\psi_{fd}/dt \quad 11$$

$$V_{kd1} = R_{kd1} I_{kd1} + d\psi_{kd1}/dt \quad 12$$

$$V_{kq1} = R_{kq1} I_{kq1} + d\psi_{kq1}/dt \quad 13$$

$$V_{kq2} = R_{kq2} I_{kq2} + d\psi_{kq2}/dt \quad 14$$

$$T_e = \psi_{ds} I_{qs} - \psi_{qs} I_{ds} \quad 15$$

The energy stored in the dc-link capacitor is given in (16), while (17) provides its dynamic. E_c symbolizes the energy stored in the capacitor; C and V_c symbolize dc-link capacitance and voltage respectively; P_{gen} and P_{grid} represent instantaneous generated and grid powers.

$$E_c = 1/2 C V_c^2 \quad 16$$

$$C V_c \, dV_c/dt = P_{gen} - P_{grid} \quad 17$$

III. Problems posed by PCC voltage transients

In the beginning of wind energy participation in the grid, the wind farms would disengage from the grid in the event of voltage fluctuations. At present, the high contribution of wind power in the grid has made any disconnection undesirable. Besides, wind generators are expected to help stabilize the grid voltage when voltage fluctuations occur. The danger of retaining the WRSG engagement during voltage fluctuations is that the dc-link capacitor experiences overvoltage. This can harm the converter. This phenomenon can be explained using (17). Under normal operation, all the instantaneous power produced equals the instantaneous grid power i.e., the total power generated by the wind generator is transferred to the grid. Therefore, no extra power is injected into the dc-link capacitor and the voltage stays steady. A power disparity occurs during voltage fluctuations where not all the power produced by the generator can be exported to the grid. Hence, some extra power is injected into the dc-link capacitor. Since, E_c increases, the dc-link voltage, V_c, also increases.

In the event of a voltage sag, the active power, P_{dc1} transported to the dc-link capacitor is shown in (18). The quantity of active power in per unit values transported to the grid depends on the voltage sag as given in (19). Similarly, (20)-(21) describe the active power flow during voltage swells in per unit values.

$$P_{dc1} = (1 - V_{sag}) \, x \, P_{gen} \quad 18$$

$$P_{out1} = V_{sag} \, x \, P_{gen} \quad 19$$

$$P_{dc2} = (1 - V_{swell}) \, x \, P_{gen} \quad 20$$

$$P_{out2} = V_{swell} \, x \, P_{gen} \quad 21$$

Conventionally, the wind generator is always operated such that no reactive power is generated, even when PCC voltage fluctuations occur. However, this option is not feasible anymore as the reactive power of the wind generator full-scale converter has to augment the grid voltage by regulating the flow of reactive power. Equation (22) shows the reactive power ability of the wind generator converter. V_{q_conv} and V_{d_conv} are grid-side converter d- and q-axis voltages, while I_{d_conv} and I_{q_conv} are d- and q-axis grid-side converter currents. Conventionally, these d-q values are regulated such that $Q_{\_conv}$ is always maintained at zero.

$$Q_{conv} = V_{q\_conv} I_{d\_conv} - V_{d\_conv} I_{q\_conv} \quad 22$$

Therefore, the operating principle for improved ride-through when voltage fluctuations

occur is to maintain the dc-link voltage V_c inside an acceptable bound and preserve the grid voltage near unity value.

IV. Novel performance augmentation strategy

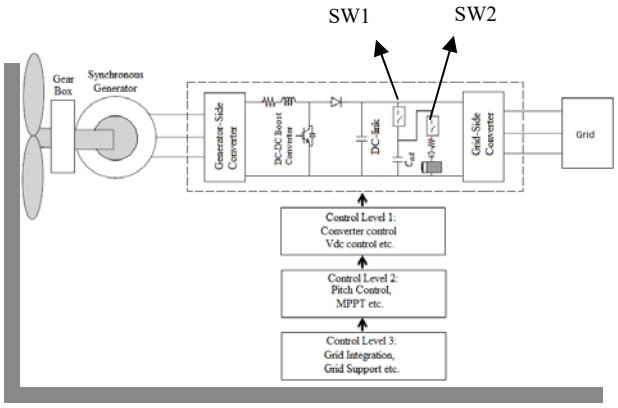

Figure 3: Novel performance strategy employed on Type 4 wind generator

A novel coordinated ride-through strategy is proposed for Type 4 wind systems to augment their operation during voltage fluctuations. The strategy includes a safety scheme and a reactive power regulation scheme. Symmetrical and asymmetrical voltage transients are included in the design of the schemes. The protection arrangement is given in Fig. 3. It includes a parallel arrangement of a NiMH battery and a supplementary capacitor, C_{ad}. The battery comprises 100 cells in series. A parallel capacitor based ride-through strategy has been utilized for DFIG wind generators but without any power storage capacity. A diode and a resistor are connected in series with the battery. The insertion of the extra capacitor and battery are regulated using switches SW1 and SW2 with the help of a supervisory (Level 3) controller. In steady state, SW1 stays open and SW2 stays closed. When voltage fluctuations occur, SW1 is closed and SW2 is opened by the supervisory controller. This inserts the capacitor C_{ad} in parallel with the dc-link capacitor, thereby increasing the total capacitance, C_{Total}, in (23). Although, the value of E_c goes up in (24), V_c stays within acceptable limits because the total capacitance increased. Hence, the converter is protected from any damage. Upon clearance of the voltage sag or swell, SW1 is opened and SW2 is closed by the supervisory controller. This enables the additional capacitor to discharge completely into the battery. Current spikes are resulting from switching is prevented by the series resistor. A diode is utilized to make sure that no energy gets transferred from the capacitor thereby discharging it. The energy accumulated in the battery is then fed back into the grid.

$$C_{Total} = C_{dc\_link} + C_{additional} \quad 23$$

$$V_c = \sqrt{(2E_c/C_{Total})} \quad 24$$

The supervisory controller (level 3 control) calculates the reactive current reference, I_{qr}, that has to be injected or consumed from the grid by the grid-side converter. The reactive power management algorithm calculates Q_{conv} in (22) to decrease the extent of PCC voltage sag or swell. The q-component of reference current, I_{q_ref}, is calculated according to a modified E.ON grid code during a sag or swell following (25)-(28) to change V_{q_conv}, which, in turn, sets the desired value of $Q_{\_conv}$. The E.ON grid code is modified for asymmetrical sags and swells because a higher quantity of reactive power supply for asymmetrical voltage sags can lead to voltage swells; and a higher absorption for asymmetrical voltage swells can cause voltage sags. The d-component of reference current, I_{d_ref}, is implemented for the dc-link voltage control and it maintains a voltage of 1100 V. The supervisory control systems use (25)-(28) to calculate the required reactive power. V_{d_conv} and V_{q_conv} are q and d-components of grid converter voltages respectively; I_{d_grid} and I_{q_grid} are d and q-components of converter currents respectively; R_{RL} and L_{RL} represent the resistance and inductance of the resistive-inductive circuit connected to the GSC respectively; K_p and K_i are the constants of PI control. Compensation terms are included in the output of the current regulators to decouple the dc-link voltage and reactive power regulations. Nevertheless, the reactive power regulation does have an impact on the dc-link voltage regulation.

$$I_{q\_grid\_ref} = 2\,x\,|V_{sym\_sag}|\ or,\ 1\,x\,|V_{asym\_sag}| \quad 25$$

$$I_{q\_grid\_ref} = -2\ x\ |V_{sym\_swell}|\ or,\ -1\ x\ |V_{asym\_swell}| \quad 26$$

$$V_{d\_conv} = -(I_{d\_grid\_ref} - I_{d\_grid})(K_p+K_i\int dt)+V_d+ I_{q\_grid\_ref}L_{RL}\omega-I_{d\_grid\_ref}R_{RL} \quad (27)$$

$$V_{q\_conv} = -(I_{q\_grid\_ref} - I_{q\_grid})(K_p+K_i\int dt)+V_q+ I_{d\_grid\_ref}L_{RL}\omega-I_{q\_grid\_ref}R_{RL} \quad (28)$$

A neural network predictive controller is designed for rotor speed control which, in turn, improves dc-voltage regulation. There are two steps involved in this, namely, system identification and control design. The nonlinear mechanical system of the wind generator is approximated using a neural network model. The Levenberg-Marquardt training algorithm is chosen for this paper.

The receding horizon technique is utilized for the predictive controller where the response of the plant is predicted over a definite time horizon. An optimization algorithm that calculates the desired control input by minimizing the performance criterion, J, given in (29). The horizons over which the control increments and tracking error are calculated are represented by n_1, n_2 and n_u. y_r and y_m are the desired and network model responses respectively, while u is the tentative control signal. The value of ρ is used to adjust weighting on control increments in the performance inject J. The grid-side converter control architecture of the Type 4 wind generator is given in Fig. 4.

$$J = \sum(y_r(k+j)-y_m(k+j))^2+\rho\sum(u'(k+j-1)-u'(k+j-2))^2 \quad (29)$$

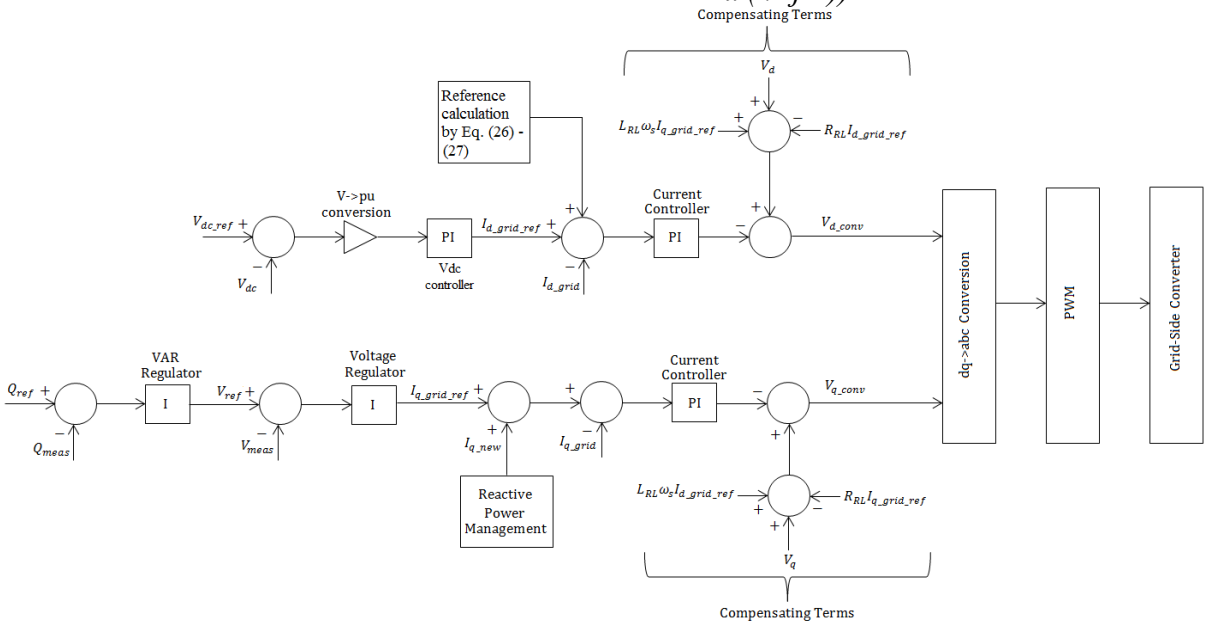

Figure 4: Grid-side converter control scheme

V. Simulation Studies

A lumped wind farm is shown in Fig. 5 which utilizes a cluster model. The wind farm symbolizes 5 x 2 MW wind generators. The farm transmits energy to the electric grid with the help of a 25 kV transmission line (30 km). A 120 KV variable voltage source symbolizes the grid of 50 Hz frequency. The wind speed is maintained at a constant value of 15 m/s. The dc-link voltage is set at 1100 V in steady state. Proportional-Integral control is implemented for the regulation of the converters. In MATLAB/Simscape Power Systems, the validity of the performance enhancement scheme is evaluated in the following scenarios: symmetrical and asymmetrical voltage sags; symmetrical and asymmetrical voltage swells. The advantage of NNPC over PI is also demonstrated.

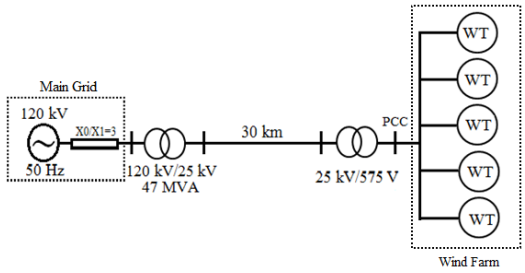

Figure 5: Test system for a 10 MW wind farm

Table: Parameters of the grid-connected wind farm

Wind turbine	H_t=4.32,H_g=0.62, K_s=0.3,D_m=1.5
Generator and converter parameters	P_{nom}=2.22MVA V_s=730V V_{dc}=1100V
NNPC parameters	N_2=7, N_u=2, ρ=0.05
Additional capacitor	C=2*C_{dc_link}
PI control parameters	$K_{p\_current}$=1, $K_{i\_current}$=50, K_{p_speed}=5, K_{i_speed}=1

A. Symmetrical voltage sag

In Fig. 6, the behaviour of Type 4 wind generators during a 30% PCC symmetrical voltage sag which lasts for 150 ms is shown with and without the novel performance augmentation strategy. Henceforth, the wind generator behaviour without the proposed strategy will be called the OFF mode, whereas the wind generator behaviour with the performance augmentation strategy will be referred to as the ON mode. The OFF and ON mode dc-link overvoltages are 1638 V and 1229 V respectively. Therefore, the novel strategy protects the converter from any damage. The supply of active power is higher in the ON mode which peaks at 0.882 p.u. compared to 0.751 p.u. in the OFF mode. Also, there is greater reactive power supply in the ON mode at 0.279 p.u., while it is kept at 0 p.u. in the OFF mode. Consequently, the magnitude of voltage sag is reduced to 0.80 p.u. in the ON mode from the OFF mode value of 0.68 p.u.

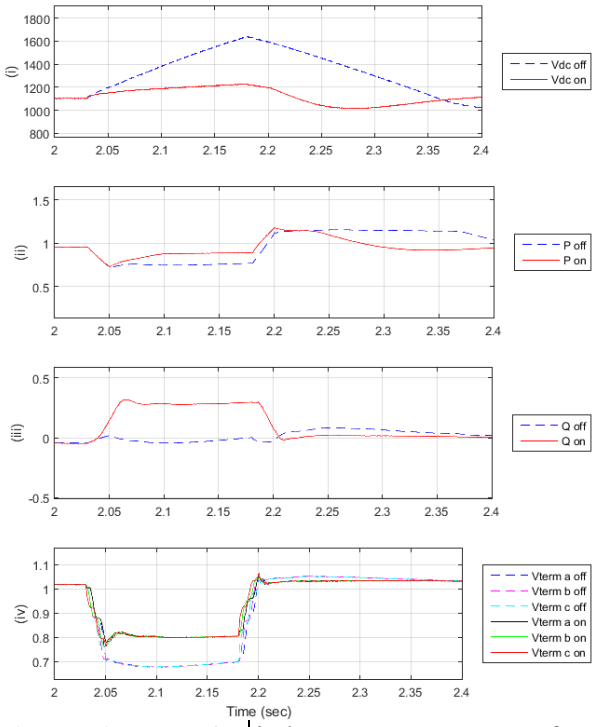

Figure 6: Type 4 wind generator response for 30% symmetrical voltage sag. (i) DC-link voltage (V). (ii) Active power (p.u.). (iii) Reactive power (p.u.). (iv) Terminal voltage (p.u.).

B. Asymmetrical voltage sag

In Fig. 7, the behaviour of Type 4 wind generators during a 30% PCC asymmetrical voltage sag which lasts for 150 ms is shown with and without the augmentation strategy. The dc-link overvoltages are 1267 V and 1147 V respectively for OFF and ON modes. Therefore, the converter is safe in the ON mode. There is a greater injection of active power in the ON mode and post-sag return to steady state value is faster. Moreover, the ON mode reactive power injection is 0.184 p.u. and OFF mode reactive power is maintained at 0 p.u. Hence, the grid voltage is supported which is apparent from the lower sag magnitude of 0.75 p.u. in ON mode compared to 0.68 p.u. OFF mode.

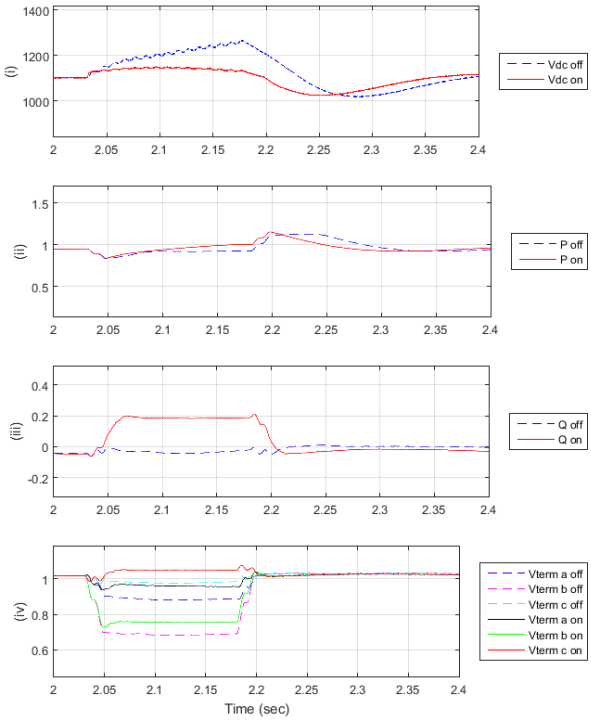

Figure 7: Type 4 wind generator response for 30% asymmetrical voltage sag. (i) DC-link voltage (V). (ii) Active power (p.u.). (iii) Reactive power (p.u.). (iv) Terminal voltage (p.u.).

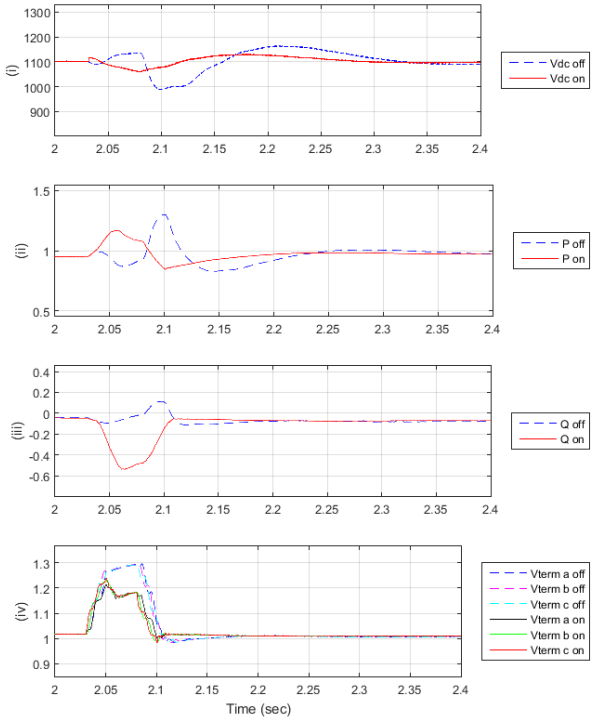

Figure 8: Type 4 wind generator response for 30% symmetrical voltage swell. (i) DC-link voltage (V). (ii) Active power (p.u.). (iii) Reactive power (p.u.). (iv) Terminal voltage (p.u.).

C. Symmetrical voltage swell

In Fig. 8, the behaviour of Type 4 wind generator during a 30% PCC symmetrical voltage swell which lasts for 50 ms is presented with and without the augmentation strategy. The OFF and ON mode dc-link undervoltages are 1137 V and 989 V respectively; while the corresponding post-swell OFF and ON mode undervoltages are 1117 V and 1058 V. Hence, the converter is secure in the ON mode and the post-swell return to steady-state is faster. There is a higher active power supply of 1.166 p.u. in ON mode compared to 0.869 p.u. in OFF mode. Also the post-swell return to steady-state is faster in ON mode. Moreover, the reactive power absorption is -0.538 p.u. in ON mode, while it is 0 p.u. in OFF mode. As a result, the grid voltage swell is reduced to 1.17 p.u. in ON mode from the OFF mode value of 1.29 p.u.

D. Asymmetrical voltage swell

In Fig. 9, the behaviour of Type 4 wind generator during a 30% PCC asymmetrical voltage swell lasting for 50 ms is shown with and without the performance augmentation strategy. The dc-link undervoltages are 1056 V and 1086 V for OFF and ON modes in that order. Hence, ON mode is closer to the steady-state value of 1100 V. Also, the post-swell return to steady state is faster in ON mode. The ON mode active power injection is 1.065 p.u. while it is 1.026 p.u. in OFF mode. Furthermore, the reactive power absorption is -0.314 p.u. in ON mode compared to 0 p.u. in OFF mode. This augments the PCC voltage by reducing the voltage swell to 1.223 p.u. in ON mode from 1.283 p.u. in OFF mode.

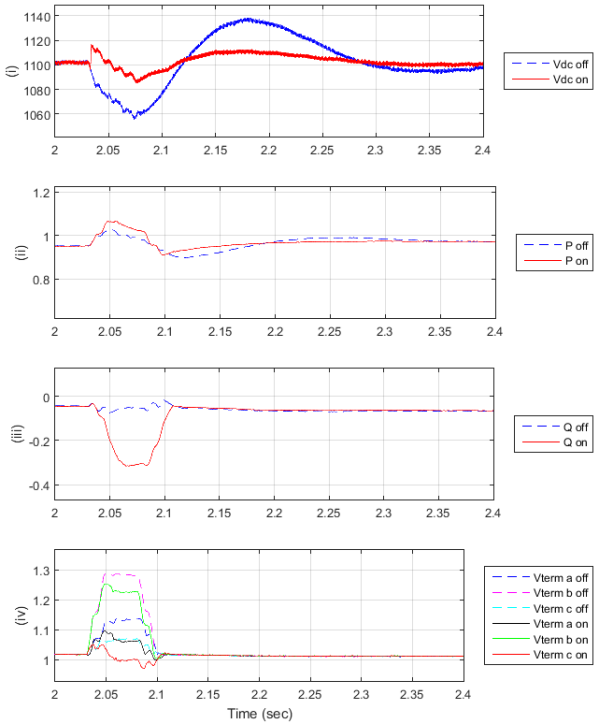

Figure 9: Type 4 wind generator response results for 30% asymmetrical voltage. (i) DC-link voltage (V). (ii) Active power (p.u.). (iii) Reactive power (p.u.). (iv) Terminal voltage (p.u.).

E. NNPC performance evaluation

In Fig. 10, the performance of the PI and NNPC in terms of dc-link voltage regulation is shown under four different PCC voltage scenarios. In this case, the reactive power management and the protection system are turned off to isolate the performance of the PI and NNPC. For a 30% symmetrical sag, the dc-link overvoltage is 1638 V for PI and 1577 V for NNPC. Similarly, the overvoltages are 1267 V and 1207 V for PI and NNPC in that order for a 30% asymmetrical voltage sag. In case of a 30% voltage swell, the undervoltages for PI and NNPC are 934.1 V and 951.9 V respectively, while the overvoltages are 1178 V and 1165 V for PI and NNPC in that order. Lastly, for a 30% asymmetrical voltage swell, the PI and NNPC undervoltages are 1038 V and 1046 V respectively, whereas the respective overvoltages are 1145 V and 1137 V. Thus, it is apparent that the NNPC provides far more efficient dc-link voltage regulation than PI.

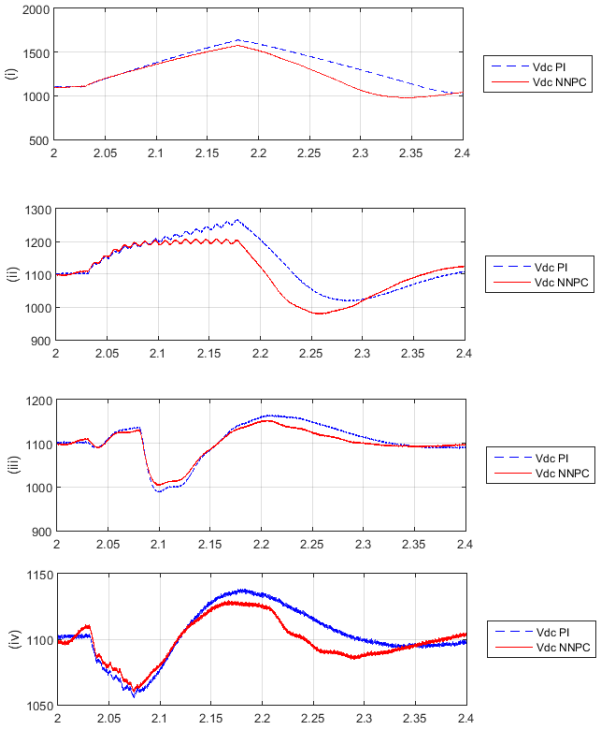

Figure 10: Performance of NNPC and PI for different PCC voltage scenarios. (i) DC-link voltage at 30% symmetrical sag (V). (ii) DC-link voltage at 30% asymmetrical sag (V). (iii) DC-link voltage at 30% symmetrical swell (V). (iv) DC-link voltage at 30% asymmetrical swell (V).

In Fig. 11, the response of the Type 4 wind generator to a disturbance in the mechanical system is shown. The reactive power management and the protection system are turned off to isolate the performance of the PI and NNPC. A step disturbance signal of magnitude 0.1 is added to the rotor speed at 1s and it steps down to zero at 1.5s. The dc-link voltage stays steady for NNPC but fluctuates between 936.6V and 1300V for PI. In case of NNPC, both active power and terminal voltage are kept at constant values of 0.9275V and 1.023 pu respectively. However, these variables show oscillatory behaviour for PI. The behaviour of reactive power is similar for both controllers but some oscillation is observed for PI control. Hence, it can be said that NNPC has the added functionality of improved wind generator performance when the mechanical system is subjected to disturbance.

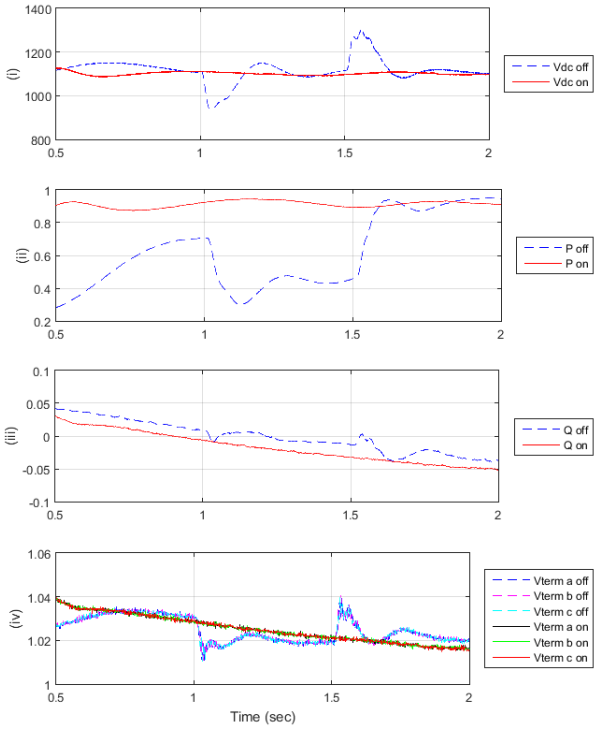

Figure 11: Type 4 wind generator simulation results for output disturbance at the mechanical system between 1s to 1.5s . (i) DC-link voltage (V). (ii) Active power (p.u.). (iii) Reactive power (p.u.). (iv) Terminal voltage (p.u.).

VI. Conclusion

This paper proposes a new performance augmentation strategy. The strategy enhances the performance of Type 4 WRSG wind generators in the event of voltage fluctuations (sags and swells). Enhanced output disturbance rejection in the mechanical system is also achieved using an NNPC which is an added advantage. The new strategy is efficient in protecting the wind generator converter by limiting the dc-link voltage inside a satisfactory range. Moreover, it supports the PCC voltage by regulating the flow of reactive power based on the type of voltage transient. This novel strategy significantly improves the grid compliance of wind generators and enables the high grid penetration of wind power to become a feasible option. Post-sag/swell effects ought to be given more attention in future work so that it becomes more inclusive. Furthermore, the active power stored in the battery should be injected back into the grid to improve system efficiency. Lastly, NNPC's could be implemented for the inner-loop current control as well.

References

A. Mullane, G. Lightboy, and R. Yacamini. 2005. "Wind-Turbine Ride-Though Enhancement." *IEEE Transactions on Power Systems* 20 (4): 1929-1937.

Akhmatov. 2006. "Modelling and Ride-through Capability of Variable Speed Wind Turbines with Permanent Magnet Generators." *Wind Energy* 9: 313 – 326.

F. Valenciaga, and R. D. Fernandez. 2015. "Multiple-input-multiple-output high-order sliding mode control for a permanent magnet synchronous generator wind-based system with grid support capabilities." *IET Renewable Power Generation* 9 (8): 925-934.

G. Ramtharan, A.Arulampalam, J.B.Ekanayake, F.M.Hughes,and N.Jenkins. 2009. "Fault ride through of fully rated converter wind turbines with AC and DC transmission systems." *IET Renewable Power Generation* 3 (4): 426 – 438.

H. Geng, G. Yang, D. Xu,and B. Wu. 2011. "(2011) 'Unified Power Control for PMSG-Based WECS Operating Under Different Grid Conditions." *IEEE Transactions on Energy Conversion* 26 (3): 822-830.

H. M. Yassin, H.H. Hanafy, and M. M. Hallouda. 2016. "Enhancement of low-voltage ride through capability of permanent magnet synchronous generator-based wind turbines using interval type-2 fuzzy control." *IET Renewable Power Generation* 10 (3): 339-348.

Hansen, A. D., and and G. Michalke. 2009. "Multi-pole permanent magnet synchronous generator wind turbines' grid support capability in uninterrupted operation during grid faults." *IET Renewable Power Generation* 3 (3): 333 – 348.

J. Dai, D. Xu, B.Wu, and N.R.Zargari. 2011. "Unified DC-Link Current Control for Low-Voltage Ride-Through in Current-Source-Converter-Based Wind Energy Conversion Systems." *IEEE Transactions on Power Electronics* 26 (1): 288 – 297.